

## Reversible Photoionization in Liquid Solutions

A. I. Burshtein\*

Department of Chemical Physics, Weizmann Institute of Science, 76100, Rehovot, Israel

K. L. Ivanov

International Tomography Center, and Novosibirsk State University, Novosibirsk, 630090, Russia

Received: August 31, 2000; In Final Form: November 13, 2000

The Stern–Volmer constant of fluorescence quenching by reversible intermolecular charge transfer is obtained by means of integral encounter theory. The latter provides the first non-Markovian description of the phenomenon which accounts for the reversibility of excited-state ionization. The forward and backward electron transfers (bimolecular and geminate) are specified by the position-dependent rates of ionization and recombination. Assuming that the conventional free energy gap law is inherent to all of them, a reasonable explanation is given for the famous Rehm and Weller free energy dependence of the Stern–Volmer constant. It requires the production of ions in excited states when forward electron transfer is highly exergonic and implies that the charge recombination occurs not only to the ground but also to the excited triplet state. It is assumed that spin conversion in the radical ion pairs is faster than the geminate recombination.

### I. Introduction

Fluorescence of the excited electron donors  $D^*$ , which may be quenched in encounters with electron acceptors A (or vice versa), is accompanied by the production of either contact or separated radical–ion pairs (RIPs). The ratio of the fluorescence quantum yield in the presence and in the absence of acceptors is known as relative quantum yield  $\eta$ , which obeys the famous Stern–Volmer law:

$$\eta = \frac{1}{1 + c \tau} \quad (1.1)$$

Here,  $c = [A]$  is the total concentration of acceptors,  $\tau$  is the lifetime of the excitation, and  $k_q$  is the Stern–Volmer quenching constant. The latter is usually studied as a function of the reaction free energy  $\Delta G_i$ , that is, the free energy of ionization  $\Delta G_i(r)$  at the closest approach distance  $r = \sigma$ . The free energy dependence ( $\Delta G_i$ ) was expected to confirm the fundamental conclusion of the Marcus theory of electron transfer, that is, the ceasing of transfer and quenching in the Marcus inverted region.<sup>1</sup> This is the region of negative  $\Delta G_i$  whose absolute values are larger than the contact reorganization energy,  $\lambda_c = \lambda(\sigma)$ . The failure of this expectation, discovered by Rehm and Weller for more than 60 electron donor–acceptor systems (Figure 1), created a problem.<sup>2</sup> The violation of the Marcus free energy gap (FEG) law in liquid solutions is contrasted with its comprehensive confirmation for solid systems or intramolecular reactions, where the distance between reactants is fixed.<sup>3</sup> This paradox attracted the attention of many authors,<sup>4–8</sup> but it still has not been undoubtedly explained.

An original FEG law was established for the monomolecular rate of ionization  $W_1(r)$  depending on the distance between  $D^*$  and A. A similar law should be inherent to the kinetic rate constant of forward electron transfer (ionization)  $k_f(\Delta G_i) = \int W_1(r) d^3r$  as well. However, the Stern–Volmer constant is not identical to  $k_f$ . If a reaction is controlled by diffusion,  $k_q$  is much closer to the diffusional rate constant  $k_D = 4\pi\sigma D$ , where  $D$  is

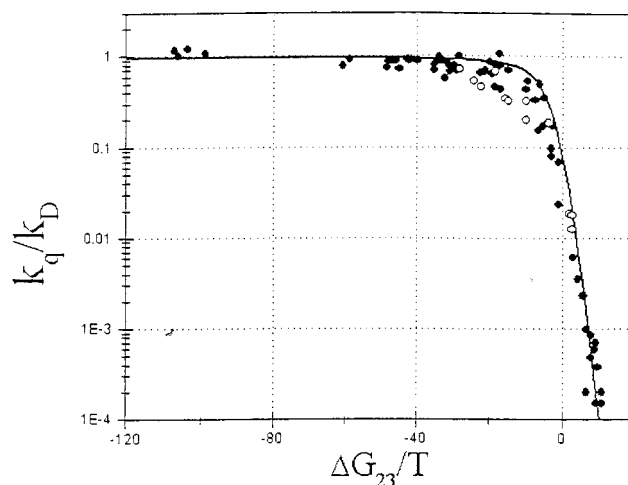


**Figure 1.** The Stern–Volmer quenching constant  $k_q \equiv k_q/k_D$  obtained in ref 2 versus the free energy of ionization  $\Delta G_{23} \equiv \Delta G_i$ . The open circles represent data obtained in another work.<sup>9</sup> The free-energy dependence, shown by a solid line, represents the theoretical expectation of Rehm and Weller deduced from their original approach to the simplest reaction mechanism of quenching.<sup>2</sup>

the sum of the diffusion coefficients of  $D^*$  and A. The diffusional rate constant establishes an upper limit for the  $k_q$ , which is independent of  $\Delta G_i$  and constitutes the plateau arising in Figure 1 at large  $|\Delta G_i|$  values. Roughly speaking, it is the same not only for different systems, but even for different reactions, provided  $D$  and  $\sigma$  are similar to all of them. The open circles in Figure 1, which were taken from another work, illustrate and enhance this statement; the whole curve is more or less universal and its interpolation, as proposed by Rehm and Weller, is still in use.<sup>9</sup>

The reverse electron transfer to the excited state with the rate  $W_B(r)$  cannot be ignored at  $\Delta G_i \geq 0$ . According to the Marcus FEG law and the detailed balance principle, the rates of

reversible electron transfer,  $W_I$  and  $W_B$ , are related to each other as follows:

$$W_I = W_i \exp\left(-\frac{(\Delta G_I + \lambda)^2}{4\lambda T}\right) = W_B \exp\left(-\frac{\Delta G_I}{T}\right) \quad (1.2)$$

where  $k_B = 1$ . At  $\Delta G_I \geq 0$  we see that  $W_B \geq W_I$  so that, in principle, backward transfer cannot be neglected. On the other hand, the rate of recombination to the ground state also obeys the same FEG law,

$$W_R = W_r \exp\left(-\frac{(\Delta G_R + \lambda)^2}{4\lambda T}\right) \quad (1.3)$$

and crucially depends on the recombination free energy

$$\Delta G_R = -\Delta G_I \quad (1.4)$$

where  $\lambda$  is the excitation energy of  $D^*$ . When  $\Delta G_I \approx 0$  we have  $\Delta G_R \approx -\lambda \gg T$  and  $W_R$  is exceptionally small. Taking an extreme view, one can conclude that sooner or later all RIPs will transform into the initial reactants and contribute to the delayed fluorescence of  $D^*$ . More precisely,  $\eta \equiv 1$  and  $\beta \equiv 0$  at  $W_R = 0$ . The reversible transfer does not work as a quenching mechanism unless the RIP recombination is much faster than reverse electron transfer to the excited state.

It is likely that only Rehm and Weller clearly understood this condition of reaching high values of  $\beta$ , thus approaching  $k_D$ . To fit the condition, they assumed that, contrary to the FEG law (1.3),

$$W_R = W_r \text{ at any } \Delta G_R \quad (1.5)$$

This is, of course, strongly inconsistent; to look for the FEG law in ionization but not in recombination. The equality (1.5) holds only in a narrow ("activationless") region, near  $\Delta G_R = -\lambda$ , but  $\Delta G_R$  does not remain constant. According to eq 1.4, it varies together with  $\Delta G_I$  over a wide range when one acceptor is substituted for another. However, surprisingly, the Rehm–Weller interpolation, based on an elementary rate description of the phenomenon and a very questionable assumption (1.5), was used a number of times, even in the most recent works, where classical dependence (1.3) was confirmed experimentally.<sup>9</sup>

Other successors of Rehm and Weller made even more rough simplifications. They assumed that ionization is irreversible, that is,  $W_B \equiv 0$ , despite the detailed balance principle (1.2) which relates  $W_B$  to  $W_I$ .<sup>4–8</sup> Although implausible, this assumption provides two significant advantages. First, it relieves one of accounting for charge recombination, which can be arbitrary slow if there is no backward transfer to the excited state. Second, the conventional differential encounter theory (DET) of irreversible transfer<sup>8,10</sup> provides the non-Markovian description of ionization kinetics via time-dependent ionization rate constant  $k_I(t)$  expressed through  $W_I(t)$ . Using DET, researchers usually concentrate on the calculation of the stationary rate constant,  $k_I = k_I(\infty)$ , fitting its free-energy dependence to the Stern–Volmer data. Generally speaking, the Stern–Volmer constant  $\neq k_I$ , but in the case of irreversible ionization there is only a small difference between them; this difference results from the non-Markovian corrections which are negligible at relatively large  $\tau$ .

The free-energy dependence  $k_I(\Delta G_I)$  is more similar to the Rehm–Weller results than to the classical FEG law particular to  $k_f(\Delta G_I)$ . When the latter was measured independently as an

initial value of the time-dependent rate constant  $k_I(0) = k_f$ , the results reproduced the bell-shaped FEG curve. In contrast, the top of the  $k_I(\Delta G_I)$  curve is cut off by the diffusional plateau  $k_I \approx k_D$ .<sup>6</sup> This is a final, commonly accepted explanation of the Rehm–Weller paradox. However, there are still two questions that remain: why the diffusional plateau is so long and why the ascending branch is so sharp. And, of course, there are no reasons, in principle, to ignore the reverse electron transfer to the excited state.

To remove this main problem, one has to substitute DET by a more general theory which accounts for reverse transfer to the excited state. This has been done recently<sup>11</sup> with the so-called integral encounter theory (IET), which provides a non-Markovian description of transfer kinetics beyond the rate concept.<sup>12</sup> IET is especially well-suited for analytic calculations of stationary characteristics of processes, like the Stern–Volmer constant. It was successfully applied to a number of similar problems in some recent works.<sup>11,13–16</sup> Here, we will calculate  $k_I(\Delta G_I)$  by means of IET and use this instead of  $k_I(\Delta G_I)$  to fit the real experimental data.

To reach results as good in agreement as those obtained by previous researchers, we have to make the forward electron transfer effectively irreversible. This is possible if the recombination of charged products at the low exergonicity edge of the FEG curve is somehow facilitated. Without resorting to eq 1.5, it can be done if ions are allowed to recombine not only to the ground state, but to the triplet state as well. The excited triplet state of neutral products is energetically much closer to the initial RIP state; therefore, the rate of recombination through this channel is much higher. The electronic excitation of RIP will also be incorporated. It is also necessary to explain fast forward transfer in the opposite edge of the FEG curve, at highly exergonic ionization. Invoking the excited states of reactants and products, we will be able to explain the whole free-energy dependence  $k_I(\Delta G_I)$ , thus circumventing revisions of the classical FEG law for backward and forward electron transfer<sup>2,17</sup> or abnormal stretching of  $\lambda(r)$  dependence.<sup>6</sup>

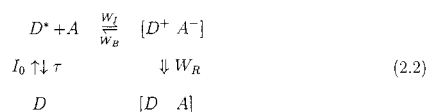
As a preliminary point, we briefly revise the problem in the next section by more accurately reproducing the Rehm–Weller estimate of  $k_I$  for reversible photoionization. This will be done in terms of the Markovian rate theory, as applied to a greatly simplified reaction scheme used in the Rehm–Weller work. In section III we will present the non-Markovian generalization of this result that is obtained with IET. Taking into account the real-space dispersion of all transfer rates and the free-ion bimolecular recombination after photoseparation, we will calculate  $k_I(\Delta G_I)$  in the most general way. In contact approximation and Markovian limit, this result reduces to the result obtained by Rehm and Weller and reproduced in section II. It will be also shown that the significant gap between the FEG law for reversible and irreversible ionization (represented by  $k_I(\Delta G_I)$ ) can be avoided if recombination to the triplet state after fast spin conversion in RIPs is taken into account. The real fitting of the IET with triple-enhanced recombination to the Rehm–Weller data is given in section IV. Using conventional space dependence of reorganization energy, we extended the diffusional plateau that covered the majority of experimental points, with the exception of a single group of the most exergonic systems. We assume that they are located at the diffusional top of another FEG curve that is related to ionization producing excited ions. In conclusion, we stress the essential, though not principal, limitations of the present theory, contact approximation and ultrafast spin conversion in RIPs.

## II. The Markovian Theory of Reversible Exciplex Formation Followed by Its Recombination

The relative quantum yield is expressed through the stationary populations of the excited and ground states,  $N_s^*$  and  $N_s$ , of fluorescent molecules permanently excited with a rate  $I_0$ .<sup>16,18</sup>

$$\eta(c) = \frac{N_s^*}{I_0 \tau N_s} \quad (2.1)$$

The stationary solution to the problem is provided by a Markovian version of DET applied to the simplest reaction scheme of Rehm and Weller.<sup>2</sup>



The full set of Markovian kinetic equations has the following form:

$$\dot{N}^* = -k_i c N^* - N^*/\tau + k_b N_e + I_0 N \quad (2.3)$$

$$\dot{N}_e = k_i c N^* - k_b N_e - W_R(\sigma) N_e \quad (2.4)$$

$$\dot{N} = -I_0 N + N^*/\tau + W_R(\sigma) N_e \quad (2.5)$$

where  $N^*$ ,  $N$ , and  $N_e$  are populations of excited and ground states and of the contact ion pair (CIP), or exciplex,  $[D^+ A^-]$ . The latter decays either back to the excited state or down to the ground state, with contact rates  $k_b$  or  $W_R(\sigma)$ , respectively. On the other hand, it is permanently generated in binary encounters of neutral reactants with the stationary rate constant of DET:<sup>10</sup>

$$k_i = \int W_I(r) n_s(r) d^3 r \quad (2.6)$$

Here,  $n_s(r)$  is the stationary solution of the auxiliary equation for reactant distribution:

$$\dot{n} = -W_I n + D \Delta n, \quad \nabla n|_{r=\sigma} = 0 \quad (2.7)$$

Setting  $\dot{N}^* = \dot{N}_e = \dot{N} = 0$  we obtain the stationary solution to the problem:

$$N_s^* = I_0 \tau N_s \left[ 1 + \frac{W_R(\sigma)}{W_R(\sigma) + k_b} k_i c \tau \right]^{-1} \quad (2.8)$$

Using this in eq 2.1, we obtain from the general formula (1.1) the following expression for the Stern–Volmer constant:

$$= \frac{k_i}{1 + k_b/W_R(\sigma)} \quad (2.9)$$

This result is identical to that which was obtained in eq 2 of the Rehm–Weller article.<sup>2</sup> The full identity is seen after untangling the relationship between the phenomenological parameters of the Rehm–Weller article and those used by DET in contact approximation:

$$k_{12} \equiv k_D = 4\pi\sigma D, \quad k_{21} = k_D/v, \quad k_{23} = W_I(\sigma) = k_f/v, \\ k_{32} = W_B(\sigma)$$

where  $v$  is the volume of the reaction zone near the contact. It should also be taken into account that in contact approximation,

$$k_i = \frac{k_f k_D}{k_f + k_D}$$

is either kinetic or diffusion controlled, as is the monomolecular rate of exciplex dissociation.<sup>19</sup>

$$k_b = W_B(\sigma) \frac{k_D}{k_f + k_D} = \frac{k_i}{Kv} \quad (2.10)$$

where

$$K = W_I(\sigma)/W_B(\sigma) = \exp(-\Delta G_i/T) \quad (2.11)$$

is the equilibrium constant of exciplex formation.

Finally, we obtain from eqs 2.9 and 2.10 that the Stern Volmer constant of reversible quenching,

$$= \frac{k_i}{1 + k_i/KW_R(\sigma)v} \quad (2.12)$$

coincides with  $k_i$  if either backward transfer to the excited state is switched off ( $K = \infty$ ) or forward transfer is irreversible due to the immediate decay of the exciplex ( $W_R(\sigma) = \infty$ ). Neither of these requests can be met at arbitrary values of  $\Delta G_i$ . If  $W_f$  and  $W_i$  are large enough, the Rehm–Weller assumption (1.5) helps the  $k_b$  and  $k_i$  values to equalize and to approach their upper limit,  $k_D$ . However, the assumption does not hold for all free energies, only near  $-\Delta G_i \approx -\lambda_c$  where recombination to the ground state is at its maximum. At large exergonicity of recombination the problem may be eliminated, but it remains very keen at  $\Delta G_i \gtrsim 0$ .

Since the plateau in Figure 1 manifests that the photoionization there is controlled by diffusion, the usage of Markovian theory is not appropriate in that region. If the ionization were irreversible one would be able to apply non-Markovian DET; this is, in essence, the rate theory, but it accounts for some nonstationary effects. Unfortunately, the rate approach to reversible reactions is invalid, especially when products are more stable than reactants.<sup>20,21</sup> Alternatively, one should apply a more fundamental non-Markovian approach, as represented by integral encounter theory (IET), which reaches beyond the rate concept and is more relevant to the problem in hand.

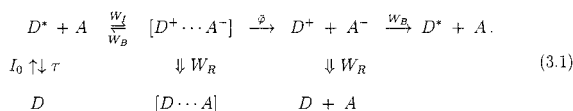
## III. The Non-Markovian Theory of Reversible Charge Separation Followed by Free Ion Recombination

Generally speaking, the exciplexes are subjected to reversible dissociation which creates the solvent-separated ion pair:  $[D^+ A^-] \rightleftharpoons [D^+ \cdots A^-]$ . The latter is mobile and can be separated in the course of diffusion into two free ions. These ions encounter the counterions from other pairs in the bulk solution and recombine with them.

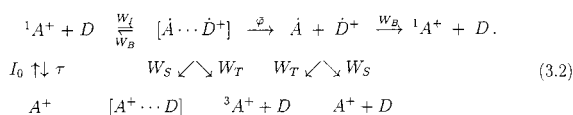
There are two alternative ways to generate an exciplex. Exciplexes can appear as a result of contact electron transfer, as in the previous section (eq 2.2), or through association of ions created by distant electron transfer (eq 3.1).<sup>22</sup> The first scheme is more reliable in nonpolar solvents, while the second is preferred in polar media. In the extreme case of highly polar solvents, where the Onsager radius  $r_c \approx \sigma$ , the depth of the Coulomb well is compatible with the thermal energy, and the exciplexes do not actually exist. The ion pairs formed in the encounters of neutral reactants appear at different distances, not always at contact. The fraction of them which escape geminate recombination and separate can be easily calculated with DET or IET. This is the charge separation quantum yield  $\bar{\varphi}$  which

determines the free ion production rate  $k_1\bar{\varphi}$ . Such a scenario, which includes the final stage of free ion recombination in a bulk, assuming the ionization is irreversible, has already been studied with IET a number of times.<sup>13–15</sup>

There was also an earlier attempt to do the same for reversible ionization, but without bimolecular recombination in the bulk.<sup>23</sup> Unfortunately, under such conditions, stationary light absorption and fluorescence do not exist; thus, eq 2.1 cannot be used for the quantum yield calculation. Therefore, we turn here to the complete scheme for the same reaction which ignores only the exciplex formation.



As a matter of fact, this alternative to the Rehm and Weller reaction (2.2) is much more plausible for distant electron transfer in highly polar solvents. In parallel, we will consider a quite different system that uses a positive ion, 2,4,6-triphenylthiopyrylium tetrafluoroborate ( $A^+$ ), as a sensitizer and a variety of halogenated benzenes, toluenes, and anisoles as electron donors (D). These systems have been studied in a few recent works,<sup>9</sup> and they were shown to participate in the following reaction:



Although this is an electron exchange reaction rather than an ionization reaction, we will not change the notation to stress the similarity. An important difference is that there are two parallel channels of RIP recombination. It was proved experimentally that this reaction results in the formation of an excited triplet of sensitizer along with its ground state, with the rates  $W_T$  and  $W_S$ , respectively.<sup>9</sup> For unknown reasons, the authors of reference 9 ignored the triplet channel in the recombination of free radicals, although they did account for it in the geminate pair. We believe that triplets should be formed with the same rate in both cases, and that their late detection can serve as an indicator of radical recombination in the bulk. Bimolecular radical recombination following the geminate recombination is naturally included in IET theory of the system response to either instantaneous or stationary excitation, launched with a rate  $I_0$ .

This is the great advantage of IET that in integral kinetic equations, as well as Markovian ones, the pumping term  $I_0N$  is additively incorporated with others. These equations, obtained recently by a regular way,<sup>11</sup> have the following form:

$$\dot{N}^* = -c \int_0^t R^*(\tau) N^*(t-\tau) d\tau + \int_0^t R^\#(\tau) [N^+(t-\tau)]^2 d\tau - \frac{N^*}{\tau} + I_0 N \quad (3.3a)$$

$$\dot{N}^+ = c \int_0^t R^\dagger(\tau) N^*(t-\tau) d\tau - \int_0^t R^\ddagger(\tau) [N^+(t-\tau)]^2 d\tau \quad (3.3b)$$

where  $N^+ = [D^+] = [A^-]$  is the total concentration of charged particles (or radicals) in solution, in pairs, and in the bulk. It was implied that the light pumping is rather weak, so that the population of the ground state  $N$  is not exhausted by the

excitation. Even more so, the pumping is unable to affect the kernels of integral equations as it does at higher light power.<sup>16,24</sup>

The kernels  $R^*$  and  $R^\dagger$  are different. The former accounts for only reversible ionization, with the forward and backward transfer rates  $W_I(r)$  and  $W_B(r)$ , while the latter takes into account, in addition, the irreversible recombination to the ground state with a rate  $W_R(r)$ . Both kernels are given by their Laplace transformations:

$$\tilde{R}^*(s) = \left( s + \frac{1}{\tau_D} \right) \int [W_I(r)\tilde{\nu}(r,s) - W_B(r)\tilde{\mu}(r,s)] d^3r \quad (3.4a)$$

$$\tilde{R}^\dagger(s) = \left( s + \frac{1}{\tau_D} \right) \int [W_I(r)\tilde{\nu}(r,s) - W_B(r)\tilde{\mu}(r,s) - W_R(r)\tilde{\mu}(r,s)] d^3r \quad (3.4b)$$

expressed via pair correlation functions  $\nu$  and  $\mu$ , which obey the auxiliary equations:

$$\dot{\nu} = -W_I(r)\nu + W_B(r)\mu - \frac{1}{\tau}\nu + D \frac{1}{r^2} \frac{\partial}{\partial r} r^2 \frac{\partial}{\partial r} \nu \quad (3.5a)$$

$$\dot{\mu} = -W_I(r)\nu - W_B(r)\mu - W_R(r)\mu + \tilde{D} \frac{1}{r^2} \frac{\partial}{\partial r} r^2 e^{r_c/r} \frac{\partial}{\partial r} e^{-r_c/r} \mu \quad (3.5b)$$

with the initial conditions  $\nu(r,0) = 1$ ,  $\mu(r,0) = 0$ , and reflecting boundary conditions. Here,  $\tilde{D}$  is an encounter diffusion coefficient for ions which may be different from that for reactants,  $D$ . The diffusional operator for ions also differs from that for neutral reactants because it accounts for the Coulomb attraction within a well of Onsager radius  $r_c$ .

The Laplace transformations of the kernels, which represent the bimolecular recombination to the ground and excited states, are

$$\tilde{R}^\ddagger(s) = s \int [W_R(r)\tilde{f}(r,s) + W_B(r)\tilde{f}(r,s) - W_I(r)\tilde{g}(r,s)] d^3r \quad (3.6a)$$

$$\tilde{R}^\#(s) = s \int [W_B(r)\tilde{f}(r,s) - W_I(r)\tilde{g}(r,s)] d^3r \quad (3.6b)$$

where auxiliary pair distributions obey the following set of equations:

$$\dot{f} = W_I(r)g - W_B(r)f - W_R(r)f + \tilde{D} \frac{1}{r^2} \frac{\partial}{\partial r} r^2 e^{r_c/r} \frac{\partial}{\partial r} e^{-r_c/r} f \quad (3.7a)$$

$$\dot{g} = -W_I(r)g + W_B(r)f - \frac{1}{\tau}g + D \frac{1}{r^2} \frac{\partial}{\partial r} r^2 \frac{\partial}{\partial r} g \quad (3.7b)$$

The initial conditions are  $f(r,0) = 1$  and  $g(r,0) = 0$ .

Setting  $\dot{N}^* = \dot{N}^+ = 0$  in eq 3.3 we obtain two algebraic equations for  $N_s$  and  $N^+$ . Resolving them for  $N_s/N$  and substituting the result into eq 2.1, we reproduce the classical Stern–Volmer law (1.1) with quenching constant

$$= \tilde{R}^*(0) \left[ 1 - \frac{\tilde{R}^\dagger(0)\tilde{R}^\#(0)}{\tilde{R}^*(0)\tilde{R}^\ddagger(0)} \right] = \begin{cases} = 0 & \text{at } W_R = 0 \\ = \tilde{R}^*(0) & \text{at } W_B = 0 \end{cases} \quad (3.8)$$

If there is no recombination to the ground state, then  $\tilde{R}^*(0) = \tilde{R}^\dagger(0)$ ,  $\tilde{R}^\#(0) = \tilde{R}^\ddagger(0)$ , and  $\tilde{R}^*(0) = 0$ . In this case, all photogenerated ions finally recombine to the excited state; this contributes to the fluorescence, and the quantum yield becomes one. Alternatively, if backward transfer to the excited state is not possible

( $W_B = 0$ ), then the general Stern–Volmer constant (3.8) reduces to the simplest expression, inherent to the irreversible photoionization.

In the normal Marcus region the electron transfer is, roughly speaking, contact.<sup>6</sup> If this is true for both the forward and backward transfer, one can set equations 1.2 and 1.3 to approximately,

$$W_i = \frac{k_f \delta(r - \sigma)}{4\pi\sigma^2}, \quad W_r = \frac{k_r \delta(r - \sigma)}{4\pi\sigma^2} \quad (3.9)$$

where

$$k_r = \int W_R(r) d^3r \quad (3.10)$$

Similarly,

$$W_B(\sigma)v \approx \int W_B(r) d^3r = k_c = k_f/K \quad (3.11)$$

in accordance with eq 2.10. In fact, either forward or backward transfer (or both) is not contact, but there is no other way to get tractable results which can be compared with elementary rate theory employed in the approach to this problem by Rehm and Weller's method.

In the contact approximation (3.9–3.11), one of the kernels,  $\tilde{R}^*(0)$ , was thoroughly studied, in ref 23, as a function of the ionization free energy  $\Delta G_i$ . Doing the same for three other kernels, we derive that

$$\begin{aligned} \tilde{R}^* &= \frac{k_f(1 + k_r \tilde{g}_2)}{Z} & \tilde{R}^\# &= \frac{k_c}{Z} & \tilde{R}^\dagger &= \frac{k_f}{Z} \\ \tilde{R}^\ddagger &= \frac{k_f + k_r + k_f k_r \tilde{g}_1}{Z} \end{aligned}$$

where

$$Z = (1 + k_f \tilde{g}_1)(1 + k_r \tilde{g}_2) + k_c \tilde{g}_2$$

Here,

$$\begin{aligned} \tilde{g}_1(s) &= [k_D(1 + \sqrt{s\tau_d + \tau_d/\tau})]^{-1}, \\ \tilde{g}_2(s) &= [k_D(1 + \sqrt{s\tau_d})]^{-1} \end{aligned} \quad (3.12)$$

where  $\tau_d = \sigma^2/D$  is an encounter time. Using these results in eq 3.8, we get the Stern–Volmer constant in the contact approximation:

$$= \frac{k_f k_r}{k_c + k_r + k_f k_r g_0} \quad (3.13)$$

where

$$g_0 = \tilde{g}_1(0) = \frac{1}{k_D(1 + \sqrt{\tau_d/\tau})} \quad (3.14)$$

If the non-Markovian contribution to the last equation,  $\sqrt{\tau_d/\tau}$ , is small (due to a long lifetime at fast diffusion) it can be neglected. Then, using  $g_0 = 1/k_D$  in eq 3.13 with eq 3.11, we can reproduce the Markovian result (2.12):

$$= \frac{k_i}{1 + k_f/Kk_r} \quad (3.15)$$

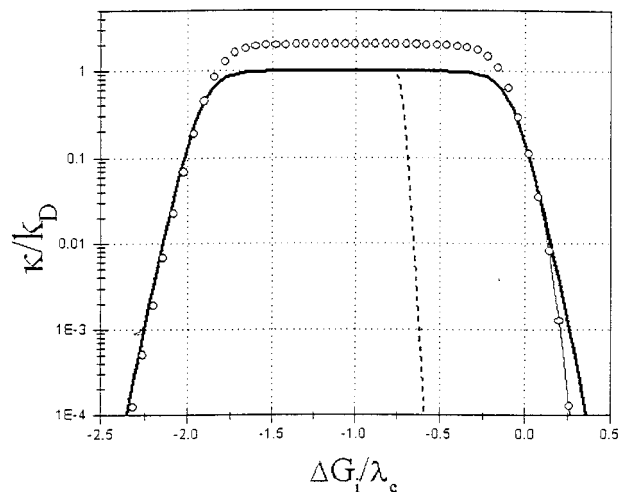


**Figure 2.** The free-energy dependence of the stationary rate constant  $k_i$  (thick line) and Markovian Stern–Volmer constants in the cases of ion recombination to the ground state (dashed line) and to the excited triplet state of products (thin line). The open circles represent the Stern–Volmer constant for the latter case, taking into account the non-Markovian effects at  $\tau = \tau_d = \sigma^2/D$ . The energy of the excited singlet state is  $\tau = 3.5\lambda_c$  and that of triplet state is  $\tau = 2.3\lambda_c$ . The maximal kinetic constant for ionization and recombination are  $k_i^{\max} \approx W_i v = 10^3 k_D$  and  $k_s^{\max} = k_T^{\max} = 0.6k_D$  ( $\lambda_c = 35T$ ).

where we took into account that in the contact approximation

$$k_i = \frac{k_f k_D}{k_f + k_D} \quad (3.16)$$

The main point is that the Stern–Volmer constant  $\tilde{R}^*$ , which is given for reversible ionization by eq 3.15, differs qualitatively from the stationary rate constant of irreversible ionization  $k_i$ , as defined by eq 3.16. However, it was the free-energy dependence of the latter that was analyzed in a number of theoretical works and fitted to the Rehm–Weller plot.<sup>4–7</sup> This is plausible where ionization is practically irreversible and  $\tilde{R}^* \approx k_i$ , but not at the right edge of this plot, at  $\Delta G_i \geq 0$ , where the sharp ascending branch is located. When  $\Delta G_i > T$ , the equilibrium constant  $K = \exp(-\Delta G_i/T) \ll 1$  while the free energy of recombination to the ground state is extremely large ( $-\Delta G_r = +\Delta G_i \gg \lambda_c$ ) and  $k_r$  is very small, according to the FEG law (1.3). Since both  $K$  and  $k_r$  are so small, we obtain from eq 3.15:

$$\approx Kk_r \ll k_i \quad (3.17)$$

This result is represented in Figure 2 by a dashed line, where  $(\Delta G_i)$  goes down too early as compared with  $k_i(\Delta G_i)$ , long before  $\Delta G_i$  turns to 0. The only way to eliminate such a crude discrepancy is to strongly facilitate the recombination at large  $\Delta G_i$ ; that was done by making an artificial Rehm–Weller assumption (1.5).

Fortunately, we can reach the same goal without breaking the fundamental FEG law (1.3), but by assuming that the neutral products of recombination can appear in excited triplet states.<sup>25</sup> The transfer to the triplet state is much less exergonic than the singlet–singlet transition to the ground state (Figure 3). This makes the total recombination much faster, and reversible ionization becomes effectively irreversible:

$$\approx k_i \text{ if } Kk_r \gg k_i \quad (3.18)$$

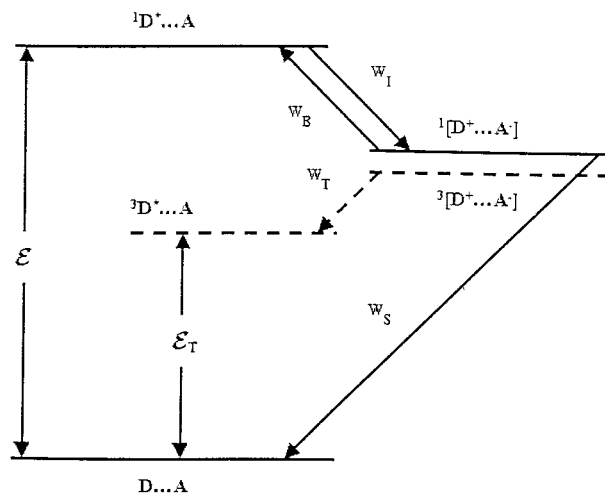


**Figure 3.** The scheme of energy levels and electron transitions in the reaction pair. Horizontal dashed lines represent triplet states of the ion pair and products of their recombination.

The mechanism which provides such an opportunity is the spin conversion in the ion pair, which makes it possible to recombine into the excited triplet state of one of the neutral products. This is exactly the same mechanism which leads to the formation of triplets in the reaction (3.2). Such a mechanism has been shown to be irreplaceable for the interpretation of the fast kinetics of ionization and charge accumulation in reaction of excited perylene with *N,N*-dimethyl-*o*-toluidine.<sup>26</sup> The recombination rates of the two competing channels have different Arrhenius factors:

$$W_S = W_r \exp\left(-\frac{(\Delta G_S + \lambda)^2}{4\lambda T}\right),$$

$$W_T = W_r \exp\left(-\frac{(\Delta G_T + \lambda)^2}{4\lambda T}\right) \quad (3.19)$$

where  $\Delta G_T = \Delta G_S + \epsilon_T$  has a much smaller absolute value than  $\Delta G_S$ . Here, we restrict our consideration to the extreme case of very fast spin-conversion in an ion-radical pair, which equilibrates the distribution over all spin states almost immediately after ionization. In this case the triplet contribution in the recombination rate  $W_R$  is maximal:

$$W_R = \frac{1}{4}W_S + \frac{3}{4}W_T \quad (3.20)$$

This generalization of the recombination rate must be combined with a substitution of  $\frac{1}{4}W_B$  for  $W_B$ .

Inclusion of the triplet channel into the recombination mechanism significantly improves the situation depicted in Figure 2. The gap between the FEG laws for reversible and irreversible ionization, which is very large for a single channel recombination (to the ground state), is removed with IET by accounting for the triplet channel. The Markovian free-energy dependence of  $k_i$  only slightly deviates from that of  $k_i$  at  $\Delta G_i > 0$ . Moreover, the ascending branch of  $k_i$  at  $\Delta G_i \approx 0$  is even sharper than that of  $k_i$ . This is actually an answer to one of the questions raised above with respect to the Rehm–Weller plot.

There are nevertheless two remarks. First of all, if one prefers to fit  $k_i(\Delta G_i)$  instead of  $k_i(\Delta G_i)$  to real experimental data, the triplet channel should be as strong as necessary to make the backward transfer negligible. Second, the difference in the lifetimes and diffusional coefficients in all reactant pairs should be negligible. In fact, the latter is hardly the truth. The ratio

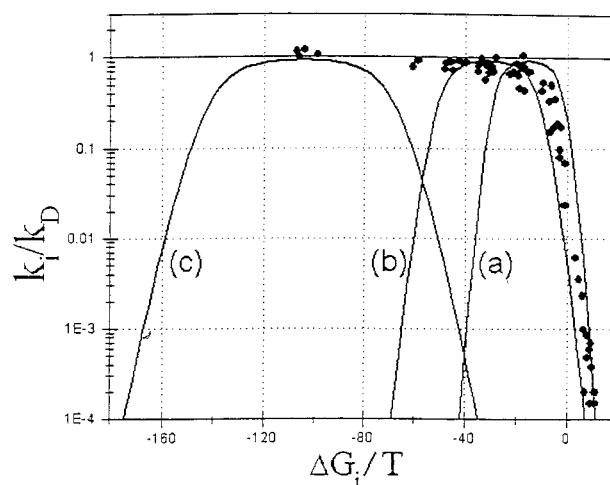


**Figure 4.** The FEG laws for the stationary ionization rate constant  $k_i(\Delta G_i)$ , obtained in the contact approximation (3.16) for three different but constant values of  $\lambda_c = 0.4$  eV (a); 0.8 eV (b); and 2.7 eV (c). The filled circles are experimental points of Rehm and Weller, taken from Figure 1.

$\tau/\tau_d$  determines the value of the non-Markovian correction to  $k_i$ , as estimated in eq 3.14. Due to this correction, the plateau in the non-Markovian theory is significantly shifted upward, as compared to the Markovian theory (Figure 2). This shift can be different for each pair of reactants because the lifetimes and diffusion coefficients are not the same for the whole collection of systems. The vertical shift of the plateau shown in Figure 2 should be considered as a measure of the spread in the experimental data for different pairs.

On this basis we will make our own fitting of the Markovian  $k_i(\Delta G_i)$  to the well-known set of Rehm–Weller experimental data below. This will be done with the contact approximation, but the quantum modes assisting electron transfer and the realistic space dependence of  $\lambda(r)$  will be taken into account.

#### IV. Fitting

As illustrated, the steep ascent to the diffusional Rehm–Weller plateau can be reached by accounting for the reverse transfer to the excited state along with the fast RIP recombination through additional triplet channels. Another problem with interpretation of Rehm–Weller results lies in the fact that the diffusional plateau, seen in Figure 1, is too wide. The same plateau inherent in the contact estimate of  $k_i(\Delta G_i)$  dependence, given by eq 3.16, is much shorter at any reasonable value of the contact reorganization energy  $\lambda_c = \lambda(\sigma)$ . In Figure 4 we compared such a dependence for three arbitrarily chosen values of  $\lambda_c$  with the original Rehm–Weller dependence. At each  $\lambda_c$  only a restricted region of the plateau can be reproduced. The latter is wider the larger the value of  $\lambda_c$ , but neither of the curves spreads the whole length of the plateau.

A few ideas have been discussed in the literature regarding how to overcome this difficulty. These take into account (i) the distance dependence of  $\lambda(r)$  in the position-dependent rate of transfer  $W(r)$ ; (ii) the multichannel nature of this rate, resulting from the assistance of the quantum mode,  $\omega$ , which is excited in the course of electron transfer; (iii) and the electronic excitation of transfer products.

In solvents of high polarity ( $\epsilon > 40$ ) one can ignore the space dispersion of free energies, assuming they are equal to the contact values everywhere ( $\Delta G_i(r) = \Delta G_i$ ). However,  $\lambda(r)$  dependence is an essential factor which affects the distant electron transfer in these solvents. With increasing exergonicity,

the rate of electron transfer takes a bell shape and shifts out of the contact.<sup>27,28</sup> Such a transformation of  $W_1(r)$  is accompanied by changing  $\lambda(r)$ , which is usually assumed to obey the classical Marcus dependence

$$\lambda(r) = \lambda_c \left( 2 - \frac{\sigma}{r} \right). \quad (4.1)$$

Since the maximum  $W_1(r)$  moves away with increasing  $\Delta G_i$ , the effective  $\lambda$  which corresponds to position of the maximum also increases with  $\Delta G_i$ . As a result, curve a shown in Figure 4 continuously transforms to curve b, whereas  $\lambda$  reaches its maximum, equal to  $2\lambda_c$ . If, for instance,  $\lambda_c = 0.4$  eV, the descending branch of a similar curve with  $\lambda_c = 0.4$  eV indicates the upper border to which a plateau may be extended due to classical  $\lambda(r)$  dependence (4.1).

This border can be shifted a little bit farther if the multichannel nature of electron transfer is involved in the fitting. In this case, the simplest single-mode formulas (1.2 and 1.3) should be substituted by the following:<sup>29</sup>

$$W_{\text{LR}}(r) = W_{\text{LR}}^0 e^{-2(r-\sigma)/L} \sum_{-\infty}^{\infty} P(n) \sqrt{\frac{T}{\lambda}} \exp \left[ -\frac{(\Delta G_{\text{LR}} + \lambda + \hbar\omega n)^2}{4\lambda T} \right], \quad (4.2)$$

where  $\Delta G_{\text{LR}} + \hbar\omega n$  is the free energy of ionization (recombination) through the  $n$ th vibronic channel and

$$P(n) = \begin{cases} e^{-S} S^n / n!, & n \geq 0 \\ \exp\left(\frac{\hbar\omega n}{T}\right) P(|n|), & n < 0 \end{cases} \quad (4.3)$$

The single Franck–Condon parameter,  $S = \lambda_q / \hbar\omega$ , is related to the quantum-mode reorganization energy  $\lambda_q$ . The higher the number of the vibronic channel, the smaller the corresponding Franck–Condon factor,  $P(n)$  at  $S \ll 1$ , which hinders remote electron transfer. However, the maxima of higher-order transitions are shifted so far away from the contact that the whole  $W_{\text{LR}}(r)$  curve and the free-energy dependence of the kinetic rate constants  $k_f(\Delta G_i) = \int W_1(r) d^3r$  or  $k_r(\Delta G_i) = \int W_R(r) d^3r$  are significantly stretched.<sup>29</sup> This is why the plateau in the  $k_i(\Delta G_i)$  dependence is also extended when transfer is assumed to be multichannel with rather high  $S$ .

The combined effect of  $\lambda(r)$  and the multichannel ionization is demonstrated in Figure 5. The dashed bell-shaped curve shows the FEG law for the single-channel contact ionization with  $\lambda_c = 0.4$  eV, which is corrected, as in Figure 2, for the backward transfer and fast recombination. The rate of the latter, shown in Figure 6, is also corrected for  $\lambda(r)$  and multichannel recombination. Composed from singlet and triplet components,  $k_r$  exceeds the value  $W_r\nu$  which is constant under the assumption made in eq 1.5. As a result, the correcting term in the denominator of eq 3.15 is small, but still essential at  $\Delta G_i \geq 0$ , where  $K \leq 1$ . Due to this term, the dependence  $k_r(\Delta G_i)$  has a steep ascent to the plateau, although  $\lambda_c$  is not as small, as it “was found to be necessary to fit the normal region of the experimental data of Rehm and Weller” with  $k_i(\Delta G_i)$ .<sup>6</sup> In fact, we used  $\lambda_c = 0.4$  eV; this is twice as large as the value used in this reference. Correspondingly, the maximal  $\lambda$  is 0.8 eV according to eq 4.1. Scanning of  $\lambda(r)$  in these limits and switching on the higher excited states of the quantum mode significantly extends the free-energy dependence of  $k_r$ , especially in the plateau region where  $k_r \approx k_D$ . The vast majority of experimental points in this

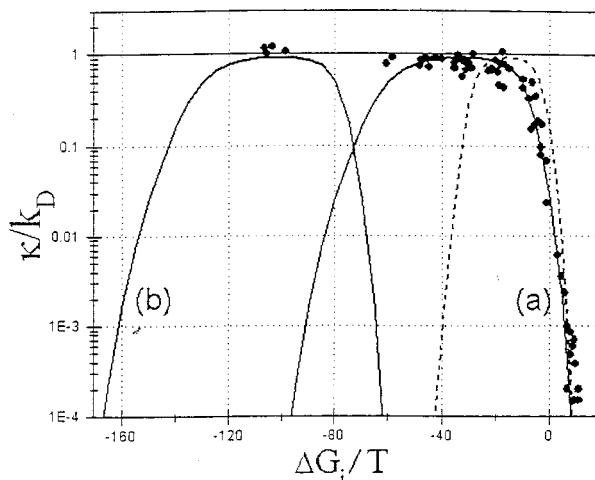


**Figure 5.** The Markovian FEG law for the Stern–Volmer constant of distant multichannel ionization (solid lines), producing stable ions (a) or electronically excited products (b) in comparison to single-channel contact ionization (dashed curve). In all cases, the backward transfer and recombination to the triplet state are taken into account. The energy of the excited singlet state of neutral reactants is  $\epsilon^* = 3.2$  eV and that of the triplet state is  $\epsilon_T = 2.7$  eV,  $\epsilon^* = 1.71$  eV,  $W_T^0 = 5 \times 10^3$  ns<sup>-1</sup>,  $W_T^0 = W_S^0 = 48$  ns<sup>-1</sup> and  $\lambda_c = 0.4$  eV;  $\omega = 0.15$  eV;  $S = 3$ ;  $L = 1.67$  Å;  $\sigma = 6$  Å; and  $k_D = 2 \times 10^{10}$  M<sup>-1</sup>s<sup>-1</sup>. The filled circles are experimental points of Rehm and Weller, taken from Figure 1.

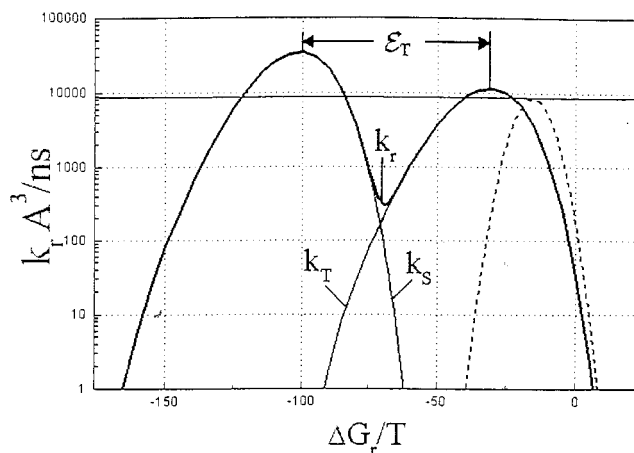


**Figure 6.** The kinetic constant for recombination at fast spin conversion,  $k_r = 1/4 k_S + 3/4 k_T$ , in comparison to  $W(\sigma)\nu$  dependence (dashed line) and the Rehm–Weller estimate (horizontal line). The thin lines represent singlet and triplet components of the total rate. The thin horizontal line represents the Rehm–Weller approximation for  $k_r$ . Here,  $\epsilon^* = 1.8$  eV;  $W_S^0 = W_T^0 = 90$  ns<sup>-1</sup>;  $\lambda_c = 0.4$  eV;  $\omega = 0.15$  eV;  $S = 3$ ;  $L = 1.67$  Å; and  $\sigma = 6$  Å.

region are covered by such a stretched FEG curve which accounts for both these effects.

Unfortunately, this stretching is not enough to extend the plateau up to a border group of points in Figure 5 with the highest exergonicity. All of them are related to donors quenched by Tetracyanoethylene (TCNE). In ref 6 they were reached by extra stretching of the FEG dependence. This was done assuming that  $\lambda(r)$  dependence differs from that of the classical law (4.1). Starting from the Monte Carlo estimates<sup>30,31</sup> of this dependence, the authors of ref 6 concluded that  $\lambda$  changes from  $\lambda_c = 0.2$  eV up to  $\lambda(\infty) = 2.7$  eV, that is, 14 instead of 2 times. We are in doubt regarding whether such a revision of eq 4.1 is well grounded and reasonable. As an alternate possibility, we would like to revive an old idea that was discussed a few times,<sup>4,32,33</sup> but then rejected for deficient reasons in ref 30. The

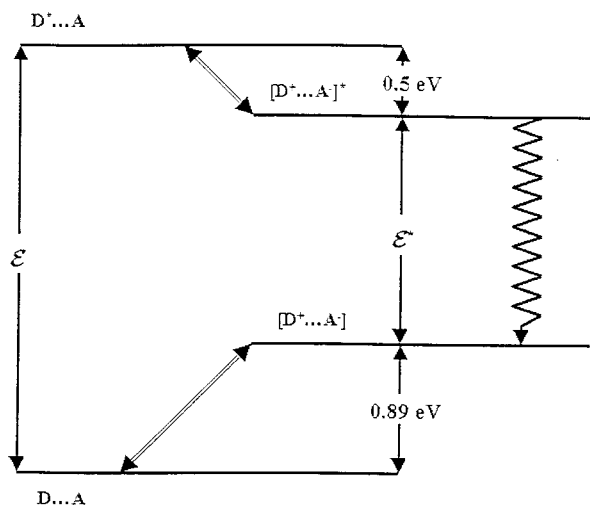


**Figure 7.** The energetic scheme with TCNE as the electron acceptor (all numerical data are taken from ref 30). The vertical wavy arrow shows the irreversible radiationless transition from the excited state to the ground state of the ion pair; inclined arrows indicate the forward and backward electron transfer;  $\epsilon = 3.1$  eV, and  $\epsilon^* = 1.71$  eV.

charge transfer complexes of TCNE with different donors have a low ground-state energy that can be formed without any excitation, though with a rather small equilibrium constant.<sup>33</sup> The energy of their excited state is also lower than that of excited reactants (Figure 7). The same is true regarding the excited states of solvent-separated ions, which we do not discriminate here from contact ion pairs (CT). The forward electron transfer into ion excited states is much faster than that into their ground states, because the corresponding free energy,  $\delta G_i = \Delta G_i - \epsilon^*$ , is significantly less than  $\Delta G_i$  in absolute value. A simple shift of our FEG curve to the left, for  $\epsilon^* = 1.71$  eV  $\approx 70 T$ , makes possible the very natural explanation of the position of TCNE points at the top of it. Since in this region  $\epsilon \approx k_D$ , all the points are located on the same plateau as the others.

This is our explanation of the abnormally wide plateau in the Rehm–Weller collection of rather dissimilar systems. Whatever these systems are, the diffusional rates are almost the same for all of them and constitute the same plateau, whose Markovian height is determined by a simple product of the diffusion coefficient and the contact radius. There are a few other collections of data which fit well with the multichannel FEG law for  $k_f(\Delta G_i)$ , without any modification of the classical  $\lambda(r)$  dependence, eq 4.1. One of them, made in ref 34, is worthy of special attention. To our knowledge, this is the single experimental observation of the Marcus inverted region, instead of a plateau, which is always obtained in liquid solutions. In this particular system (Ru<sup>II</sup> diimine complexes with cytochrome *c*), the reorganization energy is reduced, so that the kinetic rate constant pushes down and the whole FEG curve inherent to it is more narrow. However, the choice of the contact radius of 23 Å is doubtful and raises the question whether the reaction is chemically isotropic over such a huge sphere. To prove that the interpretation of the phenomenon is reliable, one needs to make one of two inspections: either to check the diffusional dependence of the FEG curve, or to measure the transient rate constant whose initial value  $k_f = k_f(0)$  should be higher than the height of the plateau  $\approx k_D$ , if electron transfer is actually controlled by diffusion. Until now such an inspection was done only for the Rehm–Weller data.<sup>6,30,35</sup> It confirms that the curve  $k_f(\Delta G_i)$  lies above the plateau and exhibits a curvature inherent to it.

## V. Conclusions

The reversibility of transfer reactions between excited particles is an insurmountable problem for a non-Markovian theory based on the rate concept.<sup>20</sup> It can be overcome only with the integral encounter theory, first used here to study the quantum yield of fluorescence quenched by reversible ionization. We argued that the fast RIPs recombination is necessary to make the reversible ionization effectively irreversible and to explain the sharp edge of the free-energy gap law in the quasi-resonant region. We assume that RIP recombination is facilitated due to spin conversion, which opens additional and more efficient channels of ion recombination to the triplet state. On the other hand, the excited triplet states of ion radicals should be produced by forward electron transfer to make it fast enough at very high exergonicity. Invoking the triplet excitations into the extended reaction scheme helps in the uniform explanation of the free-energy dependence of the Stern–Volmer constant, without revision of the classical FEG law transfer rates or space dispersion of reorganization energy.

The main limitation of the present theory is “contact approximation”. It was employed to get the relatively simple analytic solutions of our general equations and to confirm the simplest results obtained in the Rehm–Weller work, by means of conventional chemical kinetics. Sophisticated numerical programs will soon be developed for the straightforward solution of IET equations without making it necessary to resort to contact approximation. On the other hand, the viscosity dependence of the phenomenon should be studied experimentally to investigate the diffusional control of reactions in the region of the FEG plateau.

Another important limitation of the present theory is the assumption of fast spin conversion in RIPs, thus allowing the real rate and the mechanism of this process to be ignored. It may be overcome by employing a rate description of spin transitions, as in refs 36 and 37. This is appropriate for some systems in zero or relatively small external magnetic fields. Otherwise the basis of the problem should be essentially extended and a more complex theory of coherent spin transitions must be incorporated in IET, as was done for different goals in refs 38 and 39.

**Acknowledgment.** This work was supported by the Israel Science Foundation and the Karyn Kupchinet International Science School which invited K.L.I. as a summer school student, allowing him to successfully work on this paper. The numerical simulations were performed with the help of a computer program, QYield, developed by E. B. Krissinel, which was previously used for studying the spin-affected reaction of forward and backward transfer in ref 38.

## References and Notes

- (1) Marcus, R. A. *J. Chem. Phys.* **1956**, *24*, 966. Marcus, R. A. *J. Chem. Phys.* **1965**, *43*, 679.
- (2) Rehm, D.; Weller, A. *Isr. J. Chem.* **1970**, *8*, 259.
- (3) Closs, G. L.; Calcaterra, L. T.; Green, N. J.; Penfield, K. W.; Miller, J. R. *J. Chem. Phys.* **1986**, *90*, 3673.
- (4) Marcus, R. A.; Siders, P. *J. Chem. Phys.* **1982**, *86*, 622.
- (5) Tachiya, M.; Murata, S. *J. Chem. Phys.* **1992**, *96*, 8441.
- (6) (a) Kakitani, T.; Matsuda, N.; Yoshimori, A.; Mataga, N. *Prog. React. Kinet.* **1995**, *20*, 347. (b) Matsuda, N.; Kakitani, T.; Denda, T.; Mataga, N. *Chem. Phys.* **1995**, *190*, 83.
- (7) Burshtein, A. I.; Krissinel, E. B. *J. Chem. Phys.* **1996**, *100*, 3005.
- (8) Burshtein, A. I. *Adv. Chem. Phys.* **2000**, *114*, 419.
- (9) (a) Jayanthi, S. S.; Ramamurthy, P. *Phys. Chem. Chem. Phys.* **1999**, *1*, 4753. (b) Jayanthi, S. S.; Ramamurthy, P. *J. Chem. Phys.* **1998**, *102*, 511. (c) Jayanthi, S. S.; Ramamurthy, P. *J. Chem. Phys.* **1997**, *101*, 2016.
- (10) Doktorov, A. B.; Burshtein, A. I. *Sov. Phys. JETP* **1975**, *41*, 671.

- (11) Burshtein, A. I. *J. Lumin.*, in press.
- (12) (a) Sakun, V. P. *Physica A* **1975**, *80*, 128. (b) Doktorov, A. B. *Physica A* **1978**, *90*, 109. (c) Kipriyanov, A. A.; Doktorov, A. B.; Burshtein, A. I. *Chem. Phys.* **1983**, *76*, 149.
- (13) (a) Burshtein, A. I.; Frantsuzov, P. A. *J. Chem. Phys.* **1997**, *107*, 2872. (b) Burshtein, A. I.; Frantsuzov, P. A. *J. Lumin.* **1998**, *78*, 32.
- (14) Frantsuzov, P. A.; Burshtein, A. I. *J. Chem. Phys.* **1998**, *109*, 5957.
- (15) Krissinel, E. B.; Igoshin, O. A.; Burshtein, A. I. *Chem. Phys.* **1999**, *247*, 261.
- (16) Igoshin, O. A.; Burshtein, A. I. *J. Chem. Phys.* **2000**, *112*, 10930.
- (17) Agmon, N.; Levine, R. D. *Chem. Phys. Lett.* **1977**, *52*, 197.
- (18) Burshtein, A. I.; Gopich, I. V.; Frantsuzov, P. A. *Chem. Phys. Lett.* **1998**, *289*, 60.
- (19) Berg, O. G. *Chem. Phys.* **1978**, *31*, 47.
- (20) Lukzen, N. N.; Doktorov, A. B.; Burshtein, A. I. *Chem. Phys.* **1986**, *102*, 289.
- (21) (a) Burshtein, A. I.; Lukzen, N. N. *J. Chem. Phys.* **1995**, *103*, 9631. (b) Burshtein, A. I.; Lukzen, N. N. *J. Chem. Phys.* **1996**, *105*, 9588.
- (22) Burshtein, A. I. *Chem. Phys.* **1999**, *247*, 275.
- (23) Burshtein, A. I.; Frantsuzov, P. A. *J. Chem. Phys.* **1997**, *106*, 3948.
- (24) Igoshin, O. A.; Burshtein, A. I. *J. Lumin.* **2000**, *92*, 123.
- (25) Kukuchi, K.; Niwa, T.; Takahashi, Y.; Ikeda, H.; Miyashi, T. *J. Chem. Phys.* **1993**, *97*, 5070.
- (26) Burshtein, A. I.; Sivachenko, A. Yu. *Chem. Phys.* **1998**, *235*, 257.
- (27) Brunschwig, B. S.; Ehrenson, S.; Sutin, N. *J. Am. Chem. Soc.* **1984**, *106*, 6859.
- (28) Burshtein, A. I.; Frantsuzov, P. A.; Zharikov, A. A. *Chem. Phys.* **1991**, *155*, 91.
- (29) Burshtein, A. I.; Frantsuzov, P. A. *Chem. Phys.* **1996**, *212*, 137.
- (30) Kakitani, T.; Yoshimori, A.; Mataga, N. *J. Chem. Phys.* **1992**, *96*, 5385.
- (31) (a) Enomoto, Y.; Kakitani, T.; Yoshimori, A.; Hatano, Y.; Saito, M. *Chem. Phys. Lett.* **1991**, *178*, 235. (b) Enomoto, Y.; Kakitani, T.; Yoshimori, A.; Hatano, Y. *Chem. Phys. Lett.* **1991**, *186*, 366.
- (32) Mataga, N.; Kanda, Y.; Okada, T. *J. Phys. Chem.* **1986**, *90*, 3880.
- (33) Mataga, N.; Kanda, Y.; Asahi, T.; Miyasaka, H.; Okada, T.; Kakitani, T. *Chem. Phys.* **1988**, *127*, 239.
- (34) Turro, C.; Zaleski, J. M.; Karabatsos, Y. M.; Nocera, D. G. *J. Am. Chem. Soc.* **1996**, *118*, 6060.
- (35) Nishikawa, S.; Asahi, T.; Okada, T.; Mataga, N. *Chem. Phys. Lett.* **1991**, *185*, 237.
- (36) Burshtein, A. I.; Krissinel, E. *J. Phys. Chem. A* **1998**, *102*, 816, 7541.
- (37) Burshtein, A. I. *Chem. Phys.* **1999**, *247*, 275.
- (38) Krissinel, E. B.; Burshtein, A. I.; Lukzen, N. N.; Steiner, U. *Mol. Phys.* **1999**, *96*, 1083.
- (39) Burshtein, A. I.; Krissinel, E. B.; Steiner, U. *Phys. Chem. Chem. Phys.* **2001**, *3*, 198.